Experiments of closely coupled monopoles with load matching in a random field

Fei, Yuanyuan; Lau, Buon Kiong; Sunesson, Anders; Johansson, Anders J; Bach Andersen, Jørgen; Thompson, John S.

Published in:
First European Conference on Antennas and Propagation EuCAP, 2006

DOI:
10.1109/EUCAP.2006.4584482

2006

Document Version:
Peer reviewed version (aka post-print)

EXPERIMENTS OF CLOSELY COUPLED MONOPOLES WITH LOAD MATCHING IN A RANDOM FIELD

Yuanyuan Fei [1], Buon Kiong Lau [2], Anders Sunesson [3], Anders J Johansson [2], Jørgen Bach Andersen [4], and John S. Thompson [1]

[1] Institute for Digital Communications, Joint Research Institute for Signal & Image Processing, University of Edinburgh, UK. Email: y.fei@ed.ac.uk, john.thompson@ed.ac.uk

[2] Department of Electroscience, Lund University, Sweden. Email: bklau@ieee.org, anders.j.johansson@es.lth.se

[3] Perlos AB, Sweden, Email: anders.sunesson@perlos.com

[4] Department of Communications Technology, Aalborg University, Denmark. Email: jba@kom.aau.dk

ABSTRACT

Recent theoretical and simulation studies reveal that closely coupled antennas with appropriately chosen impedance matching loads can yield desired characteristics of small antenna correlation coefficients and/or high received power levels. However, no experiment has been performed to verify these claims. Here, we describe an experimental setup used to investigate the correlation and received power of closely coupled antennas with impedance matching. Specifically, a two-monopole array with a small antenna spacing 0.05 wavelength and five different matching networks are constructed and measured. Whereas our experimental results largely confirm theoretical predictions, some discrepancies due to simplifications made in the theoretical models are observed.

1. INTRODUCTION

Multiple-input multiple-output (MIMO) systems received worldwide attention in the past ten years due to their ability to significantly increase system efficiency by using multi-antennas at both ends of a wireless communication link [1]-[3]. Nevertheless, as early as in [3], it has already been mentioned the integration of MIMO technique into compact devices is restricted if the antenna spacing is below half a wavelength. This is because small antenna spacing leads to high antenna correlation and thus degradation in MIMO capacity. Moreover, strong mutual coupling (MC) between closely spaced antenna elements also results in changes in antenna patterns (thus antenna correlation) and loss of antenna efficiency [4].

Intuitively, MC is a detrimental ingredient to MIMO systems [5]. However, it is claimed in [6], [7] that MC can also be a positive factor to increase the MIMO performance under some circumstances. Recent studies [8]-[10] showed that correlation and capacity of coupled antennas can be greatly improved by introducing proper matching loads into the multiple antenna system. In [11] and [12], the relationship between various load impedances and received power/antenna correlation is carefully investigated but no measurement has been implemented to confirm the presented numerical results. On the other hand, while the S-parameters of a two-monopole array were measured and used in a related study [13], the matching networks were modeled numerically.

In this paper, a compact two- (quarter-wavelength $\lambda/4$) monopole array and five different matching networks are realized in order to experimentally verify the observed phenomena in [12]. Practical insights are presented on the role of impedance matching in the closely coupled antenna array. The paper is organized

The project is supported by VINNOVA (grant no. P24843-3), Scottish Funding Council for the Joint Research Institute with the Heriot-Watt University (a part of the Edinburgh Research Partnership), and partly conducted within the NEWCOM (Network of Excellence in Communications).

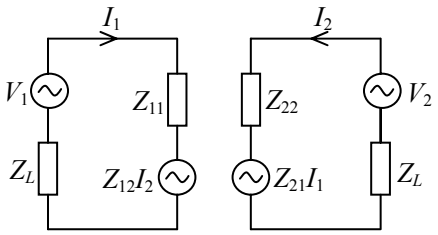

Figure 1. Equivalent circuit of two coupled antennas.

as follows. Section 2 provides the theoretical preliminaries. Section 3 focuses on the design of the overall experimental setup as well as the design of matching networks using transmission lines and open-circuit stubs. In Section 4, the simulation and experimental results are presented and discussed. Conclusions are given in Section 5.

2. THEORETICAL PRELIMINARIES

The analytical equivalent circuit for two coupled antennas is showed in Fig. 1. An identical (matching) load impedance Z_L is applied to both antennas. Z_{11}, Z_{22} and Z_{12}, Z_{21} are the self and mutual impedances of antenna 1 and 2, respectively. Meanwhile, V_1 and V_2 are open-circuit voltages as determined by the surrounding propagation environment, and they are correlated due to the small antenna spacing. Under the assumption of identical antennas, the theoretical expressions of mean received power and output correlation are derived in [12]. In practice, the relative mean received power of antenna 1 P_1 for a uniform 2D angular power spectrum (APS) can be defined by far-field antenna patterns as in Eq. 1

$$P_1 = \frac{P_{L1}}{P_0} = \frac{\int_0^{2\pi} \left|E_{L1}(\phi)\right|^2 d\phi}{\int_0^{2\pi} \left|E_0(\phi)\right|^2 d\phi}, \quad (1)$$

where P_{L1} is the power gathered by antenna 1 with load Z_L when antenna 2 is terminated with load Z_L, P_0 is the power received by a reference conjugate-matched single antenna, and $E_{L1}(\phi)$ and $E_0(\phi)$ represent the 2D far-field radiation patterns for the loaded and reference antenna cases, respectively. P_2 can be derived similarly. Eq. 2. gives the expression of the output correlation ρ, assuming uniform 2D APS where V_{L1} and V_{L2} are load voltages of antennas 1 and 2, respectively.

$$\rho = \frac{E\{V_{L1}V_{L2}^*\}}{E\{|V_{L1}|^2\}E\{|V_{L2}|^2\}} = \frac{\int_0^{2\pi} E_1(\phi)E_2^*(\phi)d\phi}{\sqrt{\int_0^{2\pi}|E_1(\phi)|^2 d\phi \int_0^{2\pi}|E_2(\phi)|^2 d\phi}}, \quad (2)$$

3. EXPERIMENTAL SETUP

3.1. System setup

The experimental setup is shown in Fig. 2. Two quarter-wavelength monopoles with antenna spacing of d = 0.05λ and 900MHz center frequency are mounted on a 330mm × 250mm ground plane. For convenience, the brass antennas of identical dimensions (thickness of 2mm) are directly soldered onto different matching network boards. The output ports are SMA connectors soldered onto the opposite end of the boards.

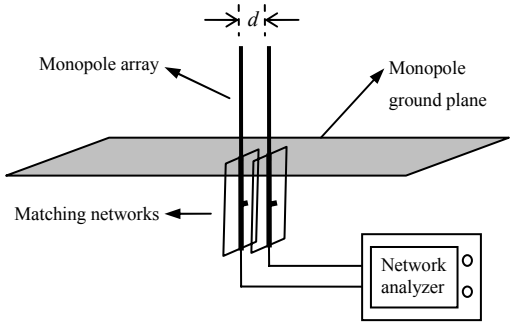

Figure 2. Experimental setup of two λ/4 monopoles mounted on a ground plane and connected to matching networks.

The self impedance of a single monopole and the self and mutual-impedances of the above monopole array are measured by a network analyzer. The network analyzer is also used for tuning the antennas with different matching boards. The 2D far-field radiation patterns of the monopole array for terminations with open-circuit and different matching networks are obtained from an anechoic chamber at Perlos AB, Sweden.

3.2. Matching network design

The design of matching networks is the vital step in the project. We apply the well established single-stub

matching technique in [14], [15]. For simplicity, the configuration of transmission line and parallel open-circuited stub based on a 50Ω transmission line is adopted.

Practically, the impedance matching networks are realized by making the appropriate microstrip transmission lines using double-side PCB boards. The width of the microstrip line is determined by the relative permittivity (ε_r) and the height (h) of the substrate layer, while the actual length design depends on the wavelength in the substrate dielectric $\lambda_e = \lambda_0/\sqrt{\varepsilon_e}$, where λ_0 is the wavelength in the free space and ε_e is defined as the effective permittivity of the dielectric interface, which can be deduced from ε_r and the width-to-height ratio w/h. A number of empirical formulas exist for w and ε_e, e.g. [14], [15], and we use those in [15].

4. MEASUREMENT AND SIMULATION RESULTS

The monopoles and ground plane are modeled in SEMCAD [16] using full-wave FDTD analysis. The impedance matrix and coupled radiation patterns are simulated for comparisons with the measurement.

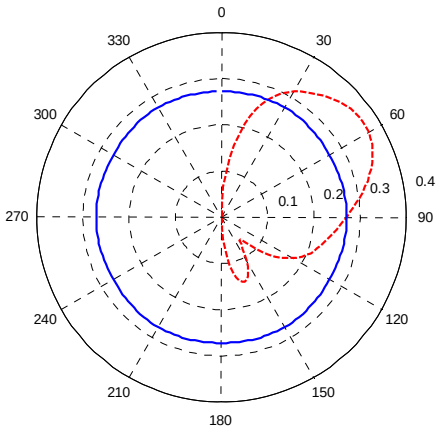

Figure 3. 2D far-field radiation patterns of single monopole. x-y plane(solid); y-z plane(dashed).

The single monopole antenna 2D far-field pattern cuts of x-y and y-z planes exported from SEMCAD are plotted in Fig. 3. As can be seen, the pattern of the azimuth plane (x-y) is almost omnidirectional, which agrees with analytical predictions. Referring to the elevation plane (y-z), an unexpected small backlobe appears under the ground plane. However, since only the pattern above the ground plane is important and the backlobe is relatively small, the backlobe has negligible impact on antenna performance. The simulated self-impedance of a single monopole Z_0 = 45.6 + j20.5 Ω agrees well with the measured impedance Z_0 = 45.5 + j19.22Ω.

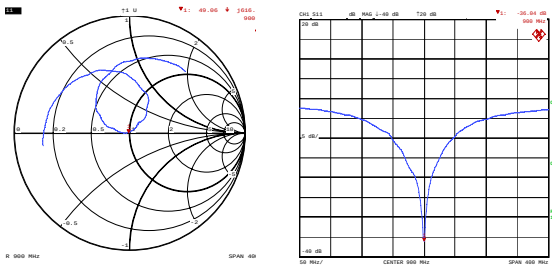

(a) (b)

Figure 4. (a). The matched impedance in Smith Chart (b). The return loss (S_{11}) of the matched monopole

To confirm the single-stub matching technique, conjugate matching for a single antenna has been attempted. From the impedance matching point of view, the input impedance of the matched antenna should be exactly 50Ω at 900MHz, i.e. the resonant frequency is tuned to 900MHz. Due to limitations in the accuracy of empirical formulas, the designed network has a resonant frequency of 897MHz. This can be easily rectified by a very small adjustment in the stub length. After a minor adjustment, the impedance (in Smith chart) and return loss read from the network analyzer are displayed in Figs. 4. In Fig. 4(b), the bandwidth is about 100MHz at -10dB return loss (or 11% fractional bandwidth).

The impedance matrix of the coupled antenna array is the most straightforward parameter to reflect the MC effect since the mutual-impedance is the outcome of the interaction between the antennas. As there are no analytical expressions for Z_{11} and Z_{12} of monopoles with finite/rectangular ground plane, both simulation and measurement results are generated. The simulated Z_{11} and Z_{12} are equal to 47.5 + j10.9Ω, 46.77 – j0.57Ω, while the measured average values are (Z_{11} + Z_{22}) /2 =

46.72 + *j*9.39Ω, $(Z_{12} + Z_{21})/2 = 45.31 - j2.57\Omega$, since ideally $Z_{11} = Z_{22}$ and $Z_{21} = Z_{12}$ for the given setup.

Besides the impedance matrix, the open-circuit correlation (ρ_{oc}) is also required to obtain the received power and output correlation from load impedances [12]. Using the open-circuit patterns from SEMCAD and Eq. 2, we obtain ρ_{oc}= 0.9796. This is close to the theoretical value for uniform 2D APS (i.e. Clarkes' model) of $\rho_{oc} = J_0(kd) = 0.9755$, where $k = 2\pi/\lambda$. Experimentally, the 2D ρ_{oc} is a complex value of 0.9473 + *j*0.0033. The imaginary part of ρ_{oc} approaches zero if the phases of the radiation patterns of the coupled antennas are symmetric about array broadside. However, it is very difficult to achieve this exactly in practice. In the case of complex valued ρ_{oc}, the total mean received power of the array should be considered instead of the mean received power of either antenna 1 or 2 as they will differ [17]. Figs. 5 and 7 display the contour plot of the total received power and output correlation utilizing the measured antenna impedances and 2D ρ_{oc} (as in [12]). Corresponding results are plotted in Figs. 6 and 8, but with the SEMCAD simulated impedances and ρ_{oc} = 0.9796. The interesting 'two maxima' phenomenon of the received power and the concentric zero output correlation contours [12] are visible in both sets of figures.

To experimentally verify the received power and correlation results in these plots, five matching load impedances (A to E) were selected from Fig. 5 and 7 (the same points are also labeled in Figs 6 and 8). The expected values at these points, as extracted from Fig. 5-8, are summarized in Tab. 1 and Tab. 2. Results from measurements performed based on the actual imple-

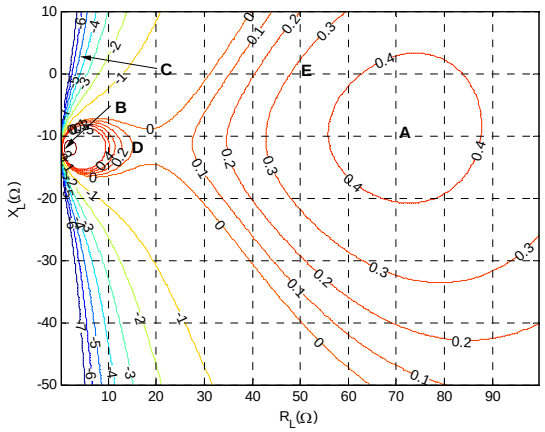

Figure 5. Numerical total power in dB as a function of Z_L with d = 0.05λ, ρ_{oc} = 0.9473 + j0.0033.

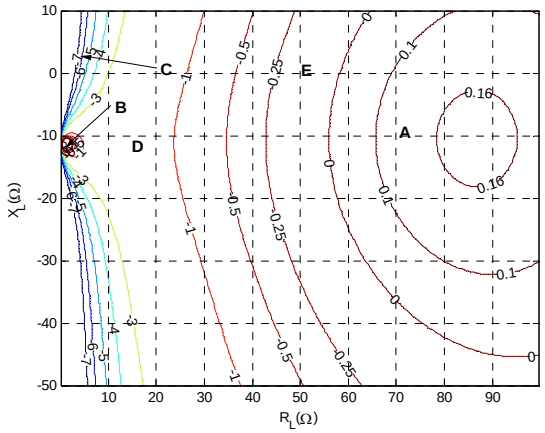

Figure 6. Numerical total power in dB vs. real and imaginary parts of Z_L with d = 0.05λ, ρ_{oc} = 0.9796.

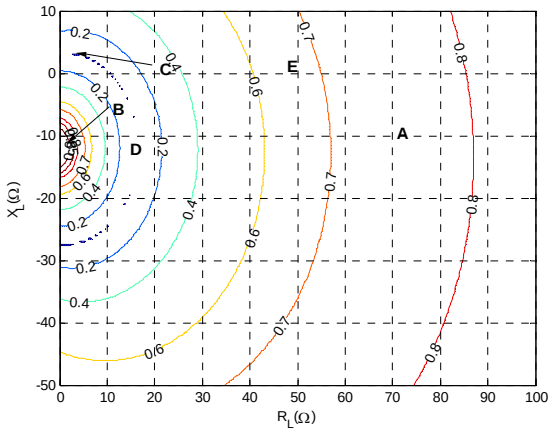

Figure 7. The output signal correlation as a function of Z_L, ρ_{oc} = 0.9473 + j0.0033.

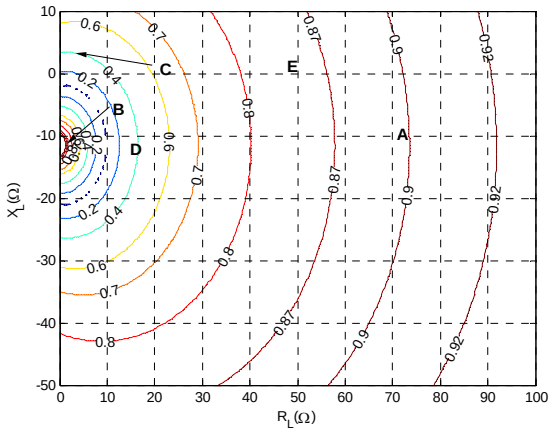

Figure 8. The output signal correlation vs. real and imaginary parts of Z_L, ρ_{oc} = 0.9796.

mentations of the selected matching impedance loads are summarized in Tab. 3.

First, we note that points A and B are chosen close to the two maxima of total received power (Fig. 5); C and D are picked from the approximately zero correlation circle (where D has the highest received power along this circle and C has a low received power of -5dB) (Figs. 5 and 7); while E is the simple 50Ω load matching as a general case.

Comparing predicted results based on measured ρ_{oc} and antenna impedances (and ideal load impedances) in Tab. 1 against directly measured results in Tab. 3, it is apparent that the measured total powers of different matching impedances generally suffer a degradation of 0.8 ~ 2.4dB except at point **B** where the gap is as large as 5.5dB. Regarding the output correlations, they are 10% higher than in Tab. 1 for most cases: at point **B** 10% lower and point **C** 30% more.

On the other hand, comparing predicted results based on simulation in Tab. 2 against directly measured results in Tab. 3, we note that the measured results agree better with the simulated results in Tab. 2 than the corresponding results in Tab. 1, except for the correlation of point D.

Moreover, it is found that the values in Tab. 2 remain almost unchanged if the measured antenna impedances (and simulated ρ_{oc}) are used instead of the simulated impedances. Taking this into consideration, and noting the some results differ considerably between Tabs. 1 and 2, we deduce that both the received power and correlation of the compact antenna array are sensitive to ρ_{oc}. Thus, the accuracy in determining ρ_{oc} (from simulated and measured open-circuit patterns) can contribute significantly to the differences between Tabs. 1 to 3, as discussed above. However, as we have seen in Figs. 5 to 8 and Tabs. 1 to 3, the two performance metrics (especially the trend) are still in general agreement between the simulated and measured cases.

The additional power loss of the directly measured case (Tab. 3) as compared to the other cases (Tabs. 1 and 2) can be partially accounted for by ohmic losses in the antennas and the matching networks. The ohmic loss is particularly severe in the case of point **B** where the predicted supergain is eliminated by high current flow. Other reasons for the discrepancies between the results (in Tabs. 1 to 3) include: (1) the sensitivity of the location of the narrow supergain peak to ρ_{oc} (see Figs. 5

Table 1. Selected load impedance for measurement with numerical total received power and correlation

	Impedances(Ω)	P_{total} (dB)	Correlation
A	70.69 - *j*9	0.4340	0.7581
B	1.5 – *j*12.8	2.5591	0.9310
C	4.06 + *j*3	-5.0000	0.0052
D	16.5 – *j*12	0.0654	0.0105
E	50 + *j*0	0.3208	0.6717

Table 2. Selected load impedance for measurement with simulated total received power and correlation

	Impedances(Ω)	P_{total} (dB)	Correlation
A	70.69 - *j*9	0.1310	0.8960
B	1.5 – *j*12.8	-0.3479	0.8668
C	4.06 + *j*3	-6.5213	0.3923
D	16.5 – *j*12	-1.4224	0.4032
E	50 + *j*0	-0.1300	0.8525

Table3. Total received power and correlation data of various load impedances in experiment

	Impedances(Ω)	P_{total} (dB)	Correlation
A	70.69 - *j*9	-0.2870	0.8541
B	1.5 – *j*12.8	-3.9977	0.7910
C	4.06 + *j*3	-7.3498	0.3681
D	16.5 – *j*12	-1.7685	0.1674
E	50 + *j*0	-0.9154	0.7800

and 6); (2) the non-ideal implementation of the matching impedance loads (even though fine-tuning was performed); (3) the accuracy of the measured complex-valued radiation patterns.

Contrasting among points **A**-**E** in Tab. 1, high received power and correlation exist for both points **A** and **B**, while **C** has the lowest correlation but also the lowest received power (or efficiency). Only point **D** provides a low correlation and a relatively high received power simultaneously. Experimentally in Tab. 3 (and likewise through simulation in Tab. 2) it is confirmed that point **D** is the preferred matching point compared to points **B** and **C** which are located in the steep gradient region for the power in Fig. 5.

5. CONCLUSION

The relative total received power and output signal correlation have been investigated numerically and experimentally by constructing a highly compact (spaced by 0.05λ) two-element $\lambda/4$ monopole array with different matching terminations. We showed that, despite some discrepancies, the measured results are generally in agreement with previous numerical analyses. The study confirms that load values could be optimized to combat performance degradation due to MC in compact antenna arrays, which improves the feasibility of incorporating MIMO techniques into small platforms.

ACKNOWLEDGEMENTS

We thank Mr. Lars Hedenstjärna of the Department of Electroscience, Lund University for technical advice and clever constructions of the experimental hardware.

6. REFERENCES

[1] J. Winters, "On the Capacity of Radio Communication Systems with Diversity in a Rayleigh Fading Environment," *IEEE J. Select. Areas Commun.*, vol. 5, pp. 871-878, Jun. 1987.

[2] I. E. Telatar, "Capacity of multi-antenna Gaussian channels," *European Trans. Telecommun*., vol. 10, pp. 585-595, 1999.

[3] G. J. Foschini and M. J. Gans, "On limits of wireless communications in a fading environment when using multiple antennas," *Wireless Personal Commun.*, vol. 6, pp. 311-335, Mar. 1998.

[4] P. S. Kildal and K. Rosengren, "Electromagnetic analysis of effective and apparent diversity gain of two parallel dipoles," *IEEE Antennas and Wireless Propagat. Lett*. , vol. 2, no. 1, pp. 9-13, 2003.

[5] M. K. Ozdemir, E. Arvas, and H. Arslan, "Dynamics of spatial correlation and implications on MIMO systems," *IEEE Commun. Magazine*, vol. 42, no. 6, pp. S14-S19, Jun. 2004.

[6] T. Svantesson, and A. Tanheim, "Mutual coupling effects on the capacity of multielement antenna systems," in *Proc. IEEE International Conference on Acoustics, Speech, and Signal Processing* (ICASSP´2001), vol. 4, pp. 2485-2488, 7-11 May 2001.

[7] V. Jungnickel, V. Pohl, and C. von Helmolt, "Capacity of MIMO systems with closely spaced antennas," *IEEE Commun. Lett.*, vol. 7, no. 8, pp. 361-363, Aug. 2003.

[8] J. W. Wallace and M. A. Jensen, "Termination-dependent diversity performance of coupled antennas: network theory analysis," *IEEE Trans. Antennas Propag*., vol. 52, no. 1, pp. 98-105, Jan. 2004.

[9] ——, "Mutual coupling in MIMO wireless systems: A rigorous network theory analysis," *IEEE Trans. Wireless Commun*., vol. 3, no. 4, pp. 1317-1325, Jul. 2004.

[10] B. K. Lau, S. M. S. Ow, G. Kristensson, and A. F. Molisch, "Capacity analysis for compact MIMO systems," in *Proc. IEEE 61st VTC Spring*, vol. 1, pp. 165-170, 2 May-1 Jun. 2005.

[11] R. G. Vaughan and J. B. Andersen, "Antenna diversity in mobile communications," *IEEE Trans. Vehic. Technol*., vol. VT-36, no. 4, pp. 149-172, Nov. 1987.

[12] J. B. Andersen and B. K. Lau, "On closely coupled dipoles in a random field," *IEEE Antennas and Wireless Propag. Lett.*, vol. 5, no. 1, pp. 73-75, 2006.

[13] S. Dossche, J. Romeu and S. Blanch, "Matching network for a spatial diversity antenna system," in *Proc. IEEE Symp. Personal Indoor and Mobile Radio Communication* (PIMRC'2004), vol. 1, pp. 427-431, 5-8 Sep. 2004.

[14] D. M. Pozar, *Microwave Engineering*, John Wiley, 1998.

[15] S. J. Orfanidis, *Electromagnetic Waves and Antennas*, http://www.ece.rutgers.edu/~orfanidi/ewa, Jun. 2004.

[16] *SEMCAD*, http://www.semcad.com.

[17] B. K. Lau and J. B. Andersen, "On closely coupled dipoles with load matching in a random field," in *Proc. IEEE Symp. Personal Indoor and Mobile Radio Communication* (PIMRC'2006), in press.